

# Molecular Genetics Evidence for the *in Vivo* Roles of the Two Major NADPH-dependent Disulfide Reductases in the Malaria Parasite<sup>\*[5]</sup>

Received for publication, April 14, 2010, and in revised form, August 27, 2010. Published, JBC Papers in Press, September 19, 2010, DOI 10.1074/jbc.M110.123323

Kathrin Buchholz<sup>‡§¶1</sup>, Elyzana D. Putrianti<sup>||</sup>, Stefan Rahlfs<sup>‡</sup>, R. Heiner Schirmer<sup>§</sup>, Katja Becker<sup>‡2</sup>, and Kai Matuschewski<sup>||3</sup>

From the <sup>‡</sup>Interdisciplinary Research Centre, Justus-Liebig University, Giessen 35390, Germany, the <sup>§</sup>Biochemistry Centre, Ruprecht-Karls University, Heidelberg 69120, Germany, the <sup>¶</sup>Department of Parasitology, Heidelberg University School of Medicine, Heidelberg 69120, Germany, and the <sup>||</sup>Parasitology Unit, Max Planck Institute for Infection Biology, Berlin 10117, Germany

Malaria-associated pathology is caused by the continuous expansion of *Plasmodium* parasites inside host erythrocytes. To maintain a reducing intracellular milieu in an oxygen-rich environment, malaria parasites have evolved a complex antioxidative network based on two central electron donors, glutathione and thioredoxin. Here, we dissected the *in vivo* roles of both redox pathways by gene targeting of the respective NADPH-dependent disulfide reductases. We show that *Plasmodium berghei* glutathione reductase and thioredoxin reductase are dispensable for proliferation of the pathogenic blood stages. Intriguingly, glutathione reductase is vital for extracellular parasite development inside the insect vector, whereas thioredoxin reductase is dispensable during the entire parasite life cycle. Our findings suggest that glutathione reductase is the central player of the parasite redox network, whereas thioredoxin reductase fulfills a specialized and dispensable role for *P. berghei*. These results also indicate redundant roles of the *Plasmodium* redox pathways during the pathogenic blood phase and query their suitability as promising drug targets for antimalarial intervention strategies.

Antioxidant enzymes play a decisive role in rapidly growing organisms, including tumor cells and pathogens. Upon a malaria infection, the protozoan parasite *Plasmodium* continuously multiplies inside host erythrocytes. This specialized lifestyle necessitates the safe management of high oxygen tension. Moreover *Plasmodium* is under constant exposure to oxidative and nitrosative stress, either generated endogenously by the high metabolic rate or produced exogenously by immune effector cells of the host in response to parasite infection (1, 2).

Reactive oxygen species (ROS)<sup>4</sup> include the superoxide anion ( $O_2^{\cdot-}$ ) formed by univalent reduction of oxygen and the hydroxyl radical ( $OH^{\cdot}$ ), which can be generated from hydrogen peroxide and the superoxide anion in the presence of iron ions. An imbalance between production and detoxification of these reactive intermediates can lead to local oxidative stress and ultimately damage vital molecules, such as proteins, lipids, or DNA.

To maintain and defend their reducing intracellular milieu, numerous organisms including malaria parasites have evolved a dual antioxidative system based on the cysteine-containing redox-active peptides glutathione (GSH) and thioredoxin (Trx) (1–3). It should be noted that this dual system also provides the reducing equivalents for converting nucleotides to deoxyribonucleotides, an essential process for DNA synthesis and rapid cell proliferation. Glutathione is the major low molecular weight antioxidant in *Plasmodium* parasites (4), and it is kept at a high level in the reduced state by the antioxidant enzyme glutathione reductase (GR) (5), which uses NADPH regenerated in the pentose phosphate pathway as an electron donor. In addition, a complete Trx system, consisting of NADPH, thioredoxin reductase (TrxR), Trx, and a number of Trx-dependent peroxidases, has been characterized in *Plasmodium* (6–8). Curiously, the malarial and related apicomplexan parasites lack catalase and a classical, selenium-containing glutathione peroxidase, two central antioxidant enzymes present in a wide range of organisms to protect themselves against hydrogen peroxide. In kinetoplastid parasites, the thioredoxin and glutathione systems are replaced by a unique redox system based on trypanothione (9, 10).

The apparent deficiency of such a unique antioxidant defense system in *Plasmodium* further underscores the central importance of the two antioxidant pathways, represented by GR and TrxR, in the parasite. Therefore, the redox metabolism in *Plasmodium* significantly differs from that of the host cells, a fundamental requirement for potential drug development (11). Specific drugs targeting these enzymes and other proteins of the *Plasmodium* redox network impair the impressive anti-ox-

\* This work was supported by grants from the Deutsche Forschungsgemeinschaft (SFB 544, B2 and B10; B1540/15-1).

[5] The on-line version of this article (available at <http://www.jbc.org>) contains supplemental Tables S1 and S2.

<sup>1</sup> Present address: Harvard School of Public Health, 665 Huntington Ave., Boston, MA 02115.

<sup>2</sup> To whom correspondence may be addressed: Interdisciplinary Research Centre, Justus-Liebig University, Heinrich-Buff-Ring 26-32, 35392 Giessen, Germany. Tel.: 49-641-9939120; Fax: 49-641-9939129; E-mail: becker.katja@gmx.de.

<sup>3</sup> To whom correspondence may be addressed: Max Planck Institute for Infection Biology, Charitéplatz 1, 10117 Berlin, Germany. Tel.: 49-30-28460535; Fax: 49-30-28460225; E-mail: matuschewski@mpiib-berlin.mpg.de.

<sup>4</sup> The abbreviations used are: ROS, reactive oxygen species; GR, glutathione reductase; GSH, glutathione; MB, methylene blue; Trx, thioredoxin; TrxR, thioredoxin reductase; RiboR, ribonucleotide reductase; TRAP, thrombospondin-related anonymous protein.

oxidative defense mechanism (12), thus rendering the parasite more susceptible to continuous oxidative attacks by the host immune response and by endogenously generated ROS. In addition, these drugs are expected to suppress DNA synthesis and cell proliferation.

In this study, we addressed the cellular roles of the two arms of the *Plasmodium* redox pathways, represented by the corresponding NADPH-dependent reductases GR and TrxR, in the rodent malaria model parasite *P. berghei*. The identification of an essential function (e.g. of *P. berghei* GR) for survival inside the mosquito vector underscores the central role in the antioxidant defense of the malaria parasite.

## EXPERIMENTAL PROCEDURES

**Experimental Animals**—Sprague-Dawley rats, NMRI mice and C57bl/6 mice were obtained from Charles Rivers Laboratories. All animal experiments were conducted in accordance with European regulations and approved by the state authorities (Regierungspräsidium Karlsruhe).

**Gene Expression Profiling**—For qRT-PCR analyses, poly(A)<sup>+</sup> RNA was isolated using oligo-dT columns (Invitrogen) from mixed blood stages, midgut- and salivary gland-associated sporozoites, and 48-h liver stages of *P. berghei* wild-type (WT) parasites. After DNase treatment, the mRNA of each sample was reversely transcribed to cDNA using oligo-dT primers (Ambion). The SYBR Green Jumpstart Taq Ready Mix (Sigma, Steinheim, Germany) was utilized for quantitative real-time PCR on the Rotor-Gene 3000 Real-Time PCR system (Corbett Research, Sydney, Australia) using gene-specific primers (supplemental Table S1). Dilution series of a cDNA-pool (1  $\mu$ l of each undiluted cDNA) with known concentrations were set as standards for each gene. Calculation of the concentration of the amplified products (ng/reaction) was based on these standards. Specificity of the amplification products was confirmed by melting curve analysis; a no-template control was added in every run. The Rotor-gene 6.0 software was used to retrieve the real time PCR results, to analyze the data, and to determine cycle threshold values. In our experiments, each RT-PCR run was carried out in triplets of one mRNA pool, and the whole series was reproduced in a second independent experiment.

**Gene Targeting Vectors and *P. berghei* Transfection**—For gene targeting *PbTrxR*, a replacement vector, *pTrxRRep*, was generated by cloning two fragments, 830 and 800 bp, into the standard transfection vector (13) using *Pb* genomic DNA as a template and the following primer combinations: *TrxR\_Rep1* for and *TrxR\_Rep1rev* for the 5'-flanking region of the *PbTrxR* locus (830 bp), and *TrxR\_Rep2for*, and *TrxR\_Rep2rev* for the 3'-flanking region (800 bp) (Supplementary Table S2).

For replacement-specific amplification of the *TrxR*(<sup>-</sup>) locus, the following primer pairs were utilized: in the 5'-region *Tgrev2* and *TrxR\_5'* testfor, and in the 3'-region *Tgfor* and *TrxR\_3'* testrev. To validate the purity of the clonal *TrxR*(<sup>-</sup>) population, a *TrxR*-specific amplification using *TrxR\_start* and *TrxR\_end* was performed (supplemental Table S2). Three independent *TrxR*(<sup>-</sup>) parasite populations were obtained. After verification of the phenotypical identity, one representative clone was used for a detailed analysis.

Similarly, a gene replacement strategy was chosen to disrupt the rodent *Plasmodium* GR gene. The two flanking regions (1,000 and 560 bp) were amplified using the following primers: *PbGR\_Rep1for* and *PbGR\_Rep1rev* for the 1,000-bp fragment, and *PbGR\_Rep2for* and *PbGR\_Rep2rev* for the 560-bp fragment using *Pb* genomic DNA as template (supplemental Table S2). Cloning into the modified transfection vector resulted in *pPbGRRep+*. *P. berghei* transfections and positive selection were done by Nucleofector technology (13). Clonal parasites were obtained by limiting dilution of single parasites into recipient NMRI mice.

Integration-specific PCR amplification of the *GR*(<sup>-</sup>) parasites was done using the following primers: *B3D+* for and *GRtest rev*, as well as *B3D+* rev and *GRtest for*. To validate the purity of the clonal *GR*(<sup>-</sup>) parasites, a *GR*-specific amplification using the primer *PbGRstart* and *PbGRend* was used for genomic DNA templates, and *GRfor* and *GRrev*, as well as *MSP1for* and *MSP1rev* for cDNA preparations (supplemental Table S2).

**Immunoblotting**—Polyclonal rabbit antibodies against *P. falciparum* glutathione reductase and thioredoxin reductase were obtained from Eurogentec (Seraing, Belgium) using highly purified recombinant proteins. The specificity of the antibodies was proven by Western blot on *P. falciparum* whole cell lysates. Rodents were infected with WT, *TrxR*(<sup>-</sup>), or *GR*(<sup>-</sup>) blood stage parasites, respectively, and cytosolic parasite proteins were extracted using 2 M urea buffer. For immunoblot analysis, proteins were separated on 10% polyacrylamide gels and transferred to nitrocellulose membranes (Bio-Rad) by electroblotting. *TrxR* (59.7 kDa) and *GR* (56.5 kDa) were detected by incubation of membranes with polyclonal anti-*P. falciparum* *TrxR* or *GR* antisera (dilution 1:1,500). Bound antibodies were detected using peroxidase-coupled anti-rabbit and anti-mouse antibodies, to detect *PbTrxR*, *PbGR*, actin, and *PbHSP70* (14), respectively. Immunostained proteins were visualized with enhanced chemoluminescence detection (Pierce). Recombinant *P. falciparum* *TrxR* was used as a positive control. The anti-*Dictyostelium discoideum* actin antiserum, which cross-reacts with apicomplexan actins, was kindly provided by Dr. Markus Meissner (Heidelberg).

**Plasmodium Life Cycle and Phenotypic Analysis of Mutant Parasites**—*Anopheles stephensi* mosquitoes were kept at 21 °C, 80% humidity, and daily feeding on 10% sucrose. Asynchronous blood-stages of *P. berghei* ANKA-GFP (WT) (14), *TrxR*(<sup>-</sup>), and *GR*(<sup>-</sup>) parasites were maintained in NMRI mice and checked for gametocyte formation and exflagellation of microgametes prior to mosquito feeding. For mosquito infection, *A. stephensi* mosquitoes were allowed to blood-feed on anesthetized mice for 15 min. Dissection of mosquitoes was conducted at days 10, 14, and 17 to determine infectivity and sporozoite numbers in midguts and salivary glands, respectively. To analyze liver stage development, sporozoites were deposited onto a semi confluent monolayer of hepatoma cells (HuH7) and incubated for 2 h, followed by washing and incubation in cell culture medium. Liver stages were detected after 48 h with a primary antibody directed against the *P. berghei* heat shock protein 70 (*PbHSP70*) (14), followed by an Alexa Fluor 488-conjugated anti-mouse antibody. To analyze sporozoite infectivity *in vivo*, Sprague-

## Plasmodium NADPH-dependent Disulfide Reductases

**TABLE 1**

Transcript levels of *P. berghei* *GR*, *TrxR*, and selected control genes during *Plasmodium* life cycle progression

Shown are mean values of triplicate measurements. The highest expression levels were set to 100%.

Gene	Sporozoites			
	Merozoites	Midgut	Salivary gland	Liver stages
<i>GR</i>	100	4.0	10.7	11.4
<i>TrxR</i>	100	3.6	0.35	16.0
<i>RiboR</i>	100	2.7	1.43	2.72
<i>TRAP</i>	0.63	100	97.7	0.47

Dawley rats were injected intravenously with 10,000 WT or *TrxR*(-) sporozoites. Parasitemia was monitored by daily blood smears. The occurrence of a single parasite marked the first day of patency.

**Determination of Total Glutathione and Free Thiols in Parasite Extracts**—Three days after infection of mice with either WT, *GR*(-), or *TrxR*(-) parasites, parasitemia was determined, mice were sacrificed, and parasites were cultured for 16–18 h to synchronize parasites. The parasites were then purified by gradient centrifugation (55% Nycodenz in PBS). After washing and final centrifugation the total parasite volume was determined taking into account cell volume and residual buffer. The suspension was mixed with 3 volumes of 5% sulfosalicylic acid, centrifuged, and the supernatant was stored at -80 °C and used for the determination of total glutathione and free thiols. The glutathione content was measured by the GR-coupled 5,5'-dithiobis-(2-nitrobenzoic acid) (DTNB)-GSH-recycling assay (15). A standard curve was prepared using appropriate concentrations of GSH and sulfosalicylic acid. The concentration of free thiols was determined spectrophotometrically on the basis of their reaction with DTNB ( $\epsilon_{412 \text{ nm}} = 13.6 \text{ mM}^{-1} \text{ cm}^{-1}$ ) (16).

## RESULTS

**Expression Profiling of Plasmodium berghei Glutathione and Thioredoxin Reductases**—We first studied mRNA levels of the two major *Plasmodium* NADPH-dependent reductases by quantitative real-time RT-PCR (Table 1). In comparison, the highest transcript levels for glutathione reductase (*GR*) and thioredoxin reductase (*TrxR*) were determined in merozoites as it is also the case for ribonucleotide reductase (*RiboR*). Abundant expression of redox enzymes is consistent with the high metabolic and multiplication rates of *Plasmodium* during blood stage development. In liver stages about 1/10 of these transcript levels were reached for *GR* and *TrxR*, i.e. 11.4 and 16%, respectively (Table 1). In the insect vector, in salivary glands the transcript level of *GR* is similarly lowered to 10.7%. *TrxR* showed only baseline expression (0.4% of maximum). In midgut the levels are comparable, 4.0% for *GR* and 3.6% for *TrxR*. For these sporozoite stages, thrombospondin-related anonymous protein (*TRAP*) was included to verify the quality of the cDNA pool. Together, expression profiling throughout the *Plasmodium* life cycle indicate potentially important and different roles for *GR* and *TrxR* in the two hosts.

**Generation of Thioredoxin Reductase Knockout Parasites**—We first investigated the *in vivo* role of the thioredoxin arm of the parasite redox network, represented by *TrxR* (gi: 68076031). Thioredoxin is the standard electron donor for

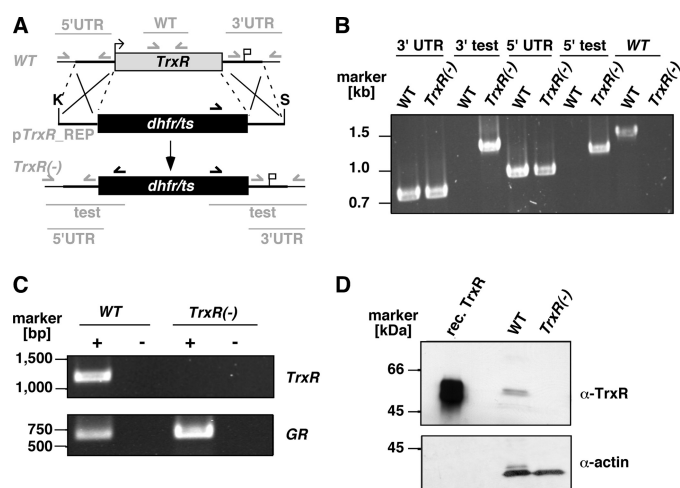


**FIGURE 1. Targeted deletion of the *P. berghei* *TrxR*.** A, replacement strategy for targeted gene disruption of *PbTrxR*. The wild-type *TrxR* locus (WT) is targeted with a KpnI (K)/SacII (S)-linearized replacement plasmid (*pTrxR* REP) containing the 5' and 3'-UTRs of *PbTrxR* and the positive selection marker *Tgdhfr/ts*. After double crossover homologous recombination, the *TrxR* open reading frame is substituted by the selection marker, resulting in the loss-of-function *TrxR*(-) allele. Replacement- and WT-specific test primer combinations and expected fragments are shown as arrows and lines, respectively. B, confirmation of the *TrxR* gene disruption by replacement-specific PCR analysis with primer combinations that amplify a signal in the recombinant locus (test) only. The absence of a WT-specific signal in the clonal *TrxR*(-) population confirms the purity of the mutant parasite line. C, depletion of *TrxR* transcripts in *TrxR*(-) parasites. cDNAs from WT and *TrxR*(-) blood stages were used as templates for *TrxR*-specific PCR reactions. Amplification of *GR* transcripts was used as a positive control. D, Western blot analysis of WT and *TrxR*(-) blood stages. Extracts from WT or *TrxR*(-) (16  $\mu$ g of total protein each) were separated on a 10% SDS gel and probed with the polyclonal anti-*PfTrxR* serum (upper panel) or a polyclonal anti-actin serum (lower panel). As a positive control 80 ng of recombinantly expressed *P. falciparum* thioredoxin reductase (rec. *TrxR*) was added.

ribonucleotide reductase and is therefore upstream of the *de novo* synthesis of deoxyribonucleotides (1–3). Previous work in the *P. falciparum* system had suggested that *PfTrxR* is vital for parasite growth under *in vitro* culture conditions (17). Toward drug target validation in the mammalian host, we targeted the *P. berghei* *TrxR* locus, employing a replacement strategy (Fig. 1A). Unexpectedly, by a single transfection attempt, we successfully integrated the *PbTrxR* disruption plasmid. This parental population was genotyped to ensure the correct replacement of the *TrxR* locus with the positive selection marker (data not shown). The population was subsequently used for the selection of clonal, *TrxR*-deficient parasite populations. We obtained three *TrxR* knockout clones, named *TrxR*(-), which exclusively showed the predicted mutant locus as verified by replacement-specific genotypic analysis (Fig. 1B). To confirm the absence of *TrxR* transcripts in *TrxR*(-) parasites, RT-PCR and subsequent cDNA synthesis were performed with poly(A)+ RNA from mixed blood stages (Fig. 1C). As predicted, no *TrxR* transcripts were detected in the knockout parasite lines, verifying the purity of the clonal populations. Moreover, Western blot analysis of *TrxR*(-) blood stages with a *PfTrxR*-specific, anti-peptide antiserum confirmed the complete absence of the protein in *TrxR*(-) parasites (Fig. 1D). This finding already indicated that *TrxR* is dispensable for the growth of asexual blood stage parasites.

**Targeted Gene Deletion of *P. berghei* Glutathione Reductase**—This finding prompted us to investigate the role of the other



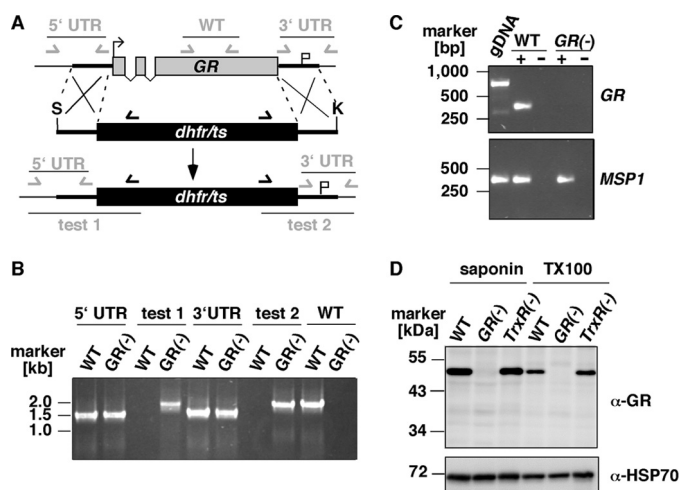


**FIGURE 2. Targeted deletion of *P. berghei* GR.** *A*, replacement strategy for targeted gene disruption of *PbGR*. The wild-type *GR* locus is targeted with a *Sac*II(*S*)/*Kpn*I(*K*)-linearized replacement plasmid containing the 5'- and 3'-UTRs of *PbGR* and the positive selection marker *Tgdhfr/ts*. After double crossover homologous recombination, the *GR* open reading frame is substituted by the selection marker, resulting in *GR* knockout parasites. Replacement-, locus-, and WT-specific test primer combinations and expected fragments are shown as arrows and lines, respectively. *B*, genotyping of the *GR*(-) disruption by PCR analysis with primer combinations that amplify signals in the recombinant locus (test 1 and 2), the *GR* locus (5'- and 3'-UTR), and the WT locus (WT). The absence of a WT-specific signal in the clonal *GR*(-) population confirms the purity of the mutant parasite line. *C*, depletion of *GR* transcripts in *GR*(-) parasites. cDNAs from WT and *GR*(-) late stage schizonts were used as templates for *GR*-specific PCR reactions. Amplification of merozoite surface protein 1 (*MSP1*) transcripts was used as a positive control. *D*, Western blot analysis of WT, *GR*(-), and *TrxR*(-) blood stages. Parasite extracts were obtained after saponin lysis (left) or Triton X-100 lysis (right) of infected erythrocytes, separated on a 10% SDS gel and probed with the polyclonal anti-*PfGR* serum (upper panel) or a monoclonal anti-*PbHSP70* antibody (lower panel). Note the absence of the *GR*-specific signal in the *GR*(-) line and comparable *GR* steady state levels in WT and *TrxR*(-) parasites.

arm of the parasite redox network, represented by GR (gi: 56499726). We first targeted the *PbGR* gene locus with an integration vector that disrupts the gene locus via a single-crossover event (data not shown). Several attempts to disrupt the gene were not successful, while an integration control that recovered the WT *GR* copy yielded recombinant parasites (data not shown). To distinguish between an essential function and difficulties in targeting the gene, we constructed a replacement vector containing the *PbGR* 5'- and 3'-untranslated regions that flank the positive selection marker cassette (Fig. 2A). Upon a double-crossover event, this vector is predicted to delete the entire *PbGR* locus. After transfection and continuous selection with the antifolate pyrimethamine, we obtained a parental population that was used for single parasite cloning. Genotyping of one clonal parasite line verified the correct gene replacement event (Fig. 2B).

To further confirm the absence of *GR* transcripts in the *GR*(-) parasites, we performed RT-PCR of cDNAs generated from blood-stage mutant and WT parasite poly(A)<sup>+</sup> RNA (Fig. 2C). As predicted, no *GR* transcripts were detected in the knockout parasites, while it was readily detectable in WT parasites. We finally tested steady state protein levels in Western blot analysis of blood stages from WT and *GR*(-) parasites (Fig. 2D). We could confirm complete depletion of *GR* in the *GR*(-) parasites. Moreover, we could show similar levels of *GR* protein in the *TrxR*(-) parasites, indicating that viability of *TrxR*(-)

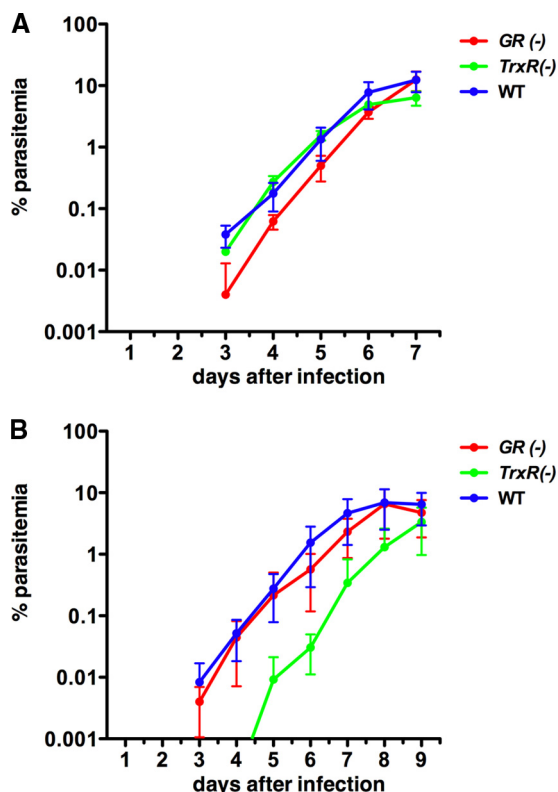


**FIGURE 3. *P. berghei* glutathione reductase and thioredoxin reductase are dispensable for asexual parasite growth.** *A*, *GR*(-) (red line) and *TrxR*(-) (green line) parasites cause high-level parasitemia *in vivo*. Displayed are *in vivo* growth curves of WT (blue lines) and knockout parasites. Five naïve animals each were injected intravenously with 1,000 asexual parasites of the respective parasite populations. Parasitemia was determined every 24 h after infection by microscopic examination of Giemsa-stained blood smears. *B*, *in vivo* growth curves of WT, *GR*(-) and *TrxR*(-) parasites under constant exposure to methylene blue (25 mg/kg/day). Treatment started immediately after infection with 1,000 WT or mutant parasite lines, respectively.

parasites is not due to compensatory up-regulation of a potential redundant gene. The successful generation of *GR*-deficient parasites already demonstrates that this gene is not essential during the pathogenic blood-stage cycle *in vivo*.

***TrxR* and *GR* Are Dispensable for Asexual Growth of *P. berghei* Blood Stages**—To test whether *GR* and/or *TrxR* serve auxiliary role(s) during blood stage infection, an *in vivo* growth assay was conducted by intravenous infection of 1,000 asexual parasites and parasitemia follow-up every 24 h after infection (Fig. 3A). Interestingly, after an initial delay in proliferation of *GR*(-) parasites, parasitemias of these and *TrxR*(-) and WT parasite lines reached comparable peak levels at day 7 after infection. This finding shows that depletion of *GR*, but not *TrxR*, may affect onset of parasite proliferation under *in vivo* growth conditions, but clearly excludes an essential function of both NADP-dependent disulfide reductases for establishment of blood stage infections.

We next wanted to determine whether loss of *GR* and/or *TrxR* function affects parasite growth *in vivo* under oxidative stress. To this end, we monitored parasitemia under enhanced stress conditions. We used methylene blue (MB) because this antimalarial had been shown to challenge the parasite's intracellular reducing milieu through the generation of pro-oxidant H<sub>2</sub>O<sub>2</sub> (18). WT-, *GR*(-)-, and *TrxR*(-)-infected mice were

## Plasmodium NADPH-dependent Disulfide Reductases

**TABLE 2**

Total glutathione concentrations in WT, *GR*(-), and *TrxR*(-) parasites

Parasite line	Total glutathione	Free thiols	<i>n</i>
	<i>mm</i>	<i>mm</i>	
WT	2.3 (± 1.1)	1.4 (± 0.8)	10
<i>GR</i> (-)	2.2 (± 0.6)	1.7 (± 0.8)	8
<i>TrxR</i> (-)	1.9 (± 0.8)	1.2 (± 0.4)	4

treated orally with 25 mg MB/kg/day. We selected this sublethal concentration, because dose finding experiments revealed rapid elimination of WT parasites with 100 mg MB/kg/day (data not shown). *In vivo* growth of the *GR*-deficient parasites, even under these enhanced oxidative stress conditions, was comparable to WT parasites (Fig. 3B). Notably, *TrxR*(-) parasites were delayed by 2 days under MB treatment, but eventually reached substantial parasitemia levels. These findings exclude central roles of *P. berghei GR* or *TrxR* in antioxidant defense.

**Total Glutathione and Non-protein-bound Free Thiols Are Unaffected in Mutant Parasites**—To test whether glutathione levels are altered in the parasite lines that lack one functional NADPH-dependent disulfide reductase we measured total glutathione concentrations in purified asexual blood stage parasites (Table 2). Total glutathione concentrations were found to be slightly, but non-significantly, lower in *GR*- and *TrxR*-deficient parasites than in the WT parasites ( $p > 0.05$ ; unpaired *t* test). Under the experimental conditions chosen, the concentrations of free thiols in the parasite extracts were determined to be 60, 79, and 62% of the total glutathione values, in WT, *GR*-, and *TrxR*-deficient cells, respectively ( $p > 0.05$ ; unpaired *t* test). Together, these data do not indicate significant alterations of parasite glutathione levels in the absence of either NADPH-dependent disulfide reductase.

***PbGR* Is Vital for Sporogony Inside the Anopheles Vector**—Previous work established that endogenous glutathione biosynthesis is critical for mosquito stage development of the malaria parasite (19). We therefore wanted to test whether *GR* displays a comparable phenotype. We infected *A. stephensi* mosquitoes with WT and *GR*(-) parasites and monitored sporogony inside the mosquito vector (Fig. 4). Whereas WT infection resulted in high densities of mature oocysts, infections with *GR*(-) parasites showed smaller oocysts (Fig. 4A). Counting oocyst numbers per infected mosquito revealed a trend toward fewer *GR*(-) oocysts compared with WT, which was, however, not significant (Fig. 4B). Quantification of midgut-associated sporozoites, the extracellular stages that are formed upon successful sporogony, revealed a complete absence of *GR*(-) sporozoites (Fig. 4C). To corroborate our results, we exposed susceptible C57bl/6 mice to 15 WT- and *GR*(-)-infected mosquitoes (WT, *n* = 3; *GR*(-), *n* = 6). As expected, none of mice exposed to *GR*(-)-infected mosquitoes developed malaria, whereas exposure to WT-infected *Anopheles* resulted in detectable parasitemia after 3 days. Together, these findings establish a vital role for *GR* during *Plasmodium* development inside the mosquito vector.

***TrxR* Is Not Necessary for the Entire Life Cycle of *P. berghei***—We finally followed the phenotype of *TrxR*(-) parasites during the entire *P. berghei* life cycle. No differences regarding game-

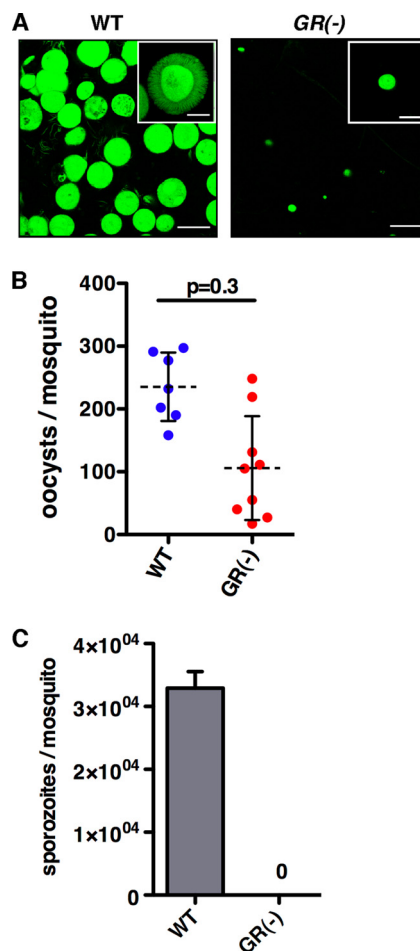


**FIGURE 4. Glutathione reductase is vital for sporogony in the mosquito vector.** A, epifluorescence micrographs of infected *A. stephensi* midguts at day 14 after an infectious bloodmeal. WT parasites mature to sporozoite-containing oocysts (left). *GR*(-) parasites colonize the mosquito midguts but are arrested in sporogony (right). Bars, 40  $\mu$ m. Insets show representative oocysts. Note the radial sporozoites emerging from the sporoblast in WT parasites. Inset bars, 16  $\mu$ m. B, quantification of oocysts per infected mosquito for WT (blue) and *GR*(-) (red) parasites. C, midgut sporozoites per infected mosquito at day 14 after feeding. WT, *n* = 7; *GR*(-), *n* = 4. No sporozoites were detectable in *GR*(-)-infected mosquitoes even after extended monitoring up to day 31.

toocyte formation, transmission to *Anopheles* mosquitoes, and oocyst development could be observed between WT and *TrxR*(-) parasites (data not shown). We next investigated sporozoite development and salivary gland invasion by comparing sporozoite numbers in infected mosquito midgut oocysts and salivary glands (Table 3). Even though the infectivity of *TrxR*(-)-infected mosquitoes and the midgut sporozoite numbers were found to be significantly lower compared with WT-infected mosquitoes, the *TrxR*-deficient parasites could apparently compensate for lower overall infection rates, since the salivary gland-associated sporozoite numbers reached levels comparable to WT parasites. Testing mature salivary gland sporozoites for *in vivo* and *in vitro* infectivity in the mammalian host revealed no striking differences between the two parasite lines. Hepatocytes infected with *TrxR*(-) sporozoites were phenotypically indistinguishable from WT-infected cells, although consistently lower numbers of mature liver stage parasites were produced (Table 3). When testing *TrxR*(-) sporo-

**TABLE 3**  
Loss of *TrxR* function does not impair *Plasmodium* life cycle progression

Parasite	Infectivity <sup>a</sup>	Midgut <sup>b</sup>	Sporozoites		Mice infected/mice inoculated (prepatent period) <sup>c</sup>	
			Salivary gland <sup>c</sup>	Liver stages <sup>d</sup>	Intravenous	By bite
<i>TrxR</i> (-) <sup>f</sup>	38% (±10%)	9,500 (±2,900)	8,250 (±1,600)	79 (±20)	7/7 (d.4)	5/5 (d.4.6)
WT	77% (±18%)	27,800 (±5,400)	12,100 (±2,200)	329 (±62)	4/4 (d.5)	6/6 (d.3.5)

<sup>a</sup> Percentage of mosquitoes that contain oocysts at days 11–13 after the infectious bloodmeal.

<sup>b</sup> Midgut-associated sporozoites per infected mosquito at days 12–14 after the infectious bloodmeal.

<sup>c</sup> Salivary gland-associated sporozoites per infected mosquito at day 17–19 after the infectious bloodmeal.

<sup>d</sup> Liver stages are represented by total numbers of mature liver stages visualized 48 h after incubation of 10,000 salivary gland sporozoites with subconfluent cultured hepatocytes.

<sup>e</sup> Prepatent period is the time until the first detection of an erythrocytic stage parasite in Giemsa-stained blood smears after intravenous injection of 10,000 salivary gland sporozoites or by bites of 5–10 infected mosquitoes.

<sup>f</sup> Two independent *TrxR*(-) clones (2 and 3) were fed. Shown are the average values from these phenotypically indistinguishable clones.

zoites *in vivo* by intravenous injection or natural mosquito bite, the recipient animals became patent after similar prepatent periods compared with WT sporozoite inoculations (Table 3). Together, our experimental genetics approach excludes an essential role for *TrxR* in any phase of the *Plasmodium* life cycle.

## DISCUSSION

To date, there is mainly biochemical and pharmacological evidence that the glutathione- and thioredoxin-based redox systems play important roles in blood stage malaria parasites (3, 20–22). As a complementation, experimental genetics in an *in vivo* model is an important tool for drug target validation. In the work described here we studied the essentiality of the two NADPH-dependent flavoenzymes glutathione reductase and thioredoxin reductase for the malaria parasite *P. berghei*. The two proteins are the principal electron donors for the glutathione and thioredoxin redox networks comprising, among others, peroxiredoxins, glyoxalases, glutathione *S*-transferase, plasmoredoxin, thioredoxins, and glutaredoxins (1, 2, 23, 24).

Using double crossover replacement, we successfully deleted the *GR* locus in *P. berghei* blood stages. *P. berghei TrxR* was also efficiently targeted by gene disruption. Interestingly, the loss of *GR* function resulted in viable and infectious blood stage malaria parasites *in vivo*. However, for sporogony in the mosquito vector *GR* was found to be essential. In contrast to previous studies on *P. falciparum* (17), *TrxR*-deficient *P. berghei* parasites could be readily obtained. A systematic phenotypic analysis of the *PbTrxR*(-) mutant throughout the *Plasmodium* life cycle excluded an essential function for *TrxR* in any of the developmental stages.

The data on *GR* depletion are supported by a recent report of Vega-Rodriguez *et al.* (19). In their study, the authors disrupted the  $\gamma$ -glutamylcysteine synthetase ( $\gamma$ -GCS) gene of *P. berghei*.  $\gamma$ -GCS is a critical component of the GSH biosynthesis pathway. Gene disruption resulted in growth retardation and depletion of GSH levels in blood stage parasites. However, like in our study on *GR*, the gene was not found to be essential. In contrast,  $\gamma$ -GCS gene disruption had a dramatic effect on the development of mosquito stages resulting in reduced numbers of stunted oocysts that did not undergo full sporogony and, therefore, failed to produce sporozoites (19). Taken together, the two studies suggest that neither the synthesis nor the *GR*-based reduction of glutathione are essential for *P. berghei* blood stages *in vivo*. This observation is in contrast to biochemical studies which demonstrated lethal effects of a  $\gamma$ -GCS inhibition by

L-buthionine sulfoximine on *P. falciparum in vitro* (21). The observed differences might be based on the different experimental approaches. However, they might also point to differences in glutathione metabolism and requirements in murine and human malaria parasites. Further studies, like knockouts of the *GR* and the  $\gamma$ -GCS genes in *P. falciparum* are required to answer this question.

As mentioned above, *GR* as well as  $\gamma$ -GCS (19) depletion lead to severe disturbance of the development of parasite mosquito stages. The discussed irreversible damage of oocyst mitochondria in  $\gamma$ -GCS depletion might point to enhanced oxidative stress based on limited availability of glutathione. Apart from different metabolic requirements, which might contribute to enhanced oxidative burden, the mosquito stages are extracellular parasite forms and thus potentially exposed to higher fluxes of reactive oxygen species. In addition, it should be kept in mind that dipteran insects including *Anopheles* and *Drosophila* do not possess a genuine glutathione reductase (6, 25). In these organisms the non-enzymatic reduction of glutathione is, at least partially, effected by reaction with reduced thioredoxin. In the WT parasite, the available enzymatic reduction of glutathione by *GR* is likely to be much more efficient than in the *GR*-deficient vector. This constellation might explain why it is impossible for a *GR*-deficient parasite to develop within a *GR*-deficient host. Another important observation is the fact that in salivary glands of mosquitoes infected with WT parasites pronounced *GR* transcripts were determined whereas *TrxR*-transcripts were hardly detectable (Table 1). This constellation points to a specific role of *GR* in mosquito stage parasites. This might also explain why the thioredoxin system cannot compensate *GR*-deficiency in these stages.

In our study *TrxR*-deficient *P. berghei* parasites were viable throughout the *Plasmodium* life cycle, although infectivity and parasite counts in the midgut and the salivary glands of the insect vector, as well as in mouse liver were reduced (Table 3). These data exclude an essential function of *TrxR* in both mammalian host and vector. Notably, in a previous experimental approach *TrxR*(-) parasites could not be obtained in cultured erythrocytes infected with a *P. falciparum* laboratory strain (17). Possible explanations for the strikingly different results include (i) frequently observed technical problems in the *P. falciparum* transfection system, (ii) an important role of *TrxR* for *Plasmodium* under *in vitro* culture conditions (which only partially reflect the physiological environment and lack feed-back regulation by the host), or (iii) a different role of *TrxR* in rodent and primate/human parasites, as also discussed above for *GR*.



## Plasmodium NADPH-dependent Disulfide Reductases

The fact that neither GR nor TrxR are essential for blood stage *P. berghei* parasites might be explained by a functional overlap between the glutathione and the thioredoxin system. The major functions of the two systems include recycling of reduced glutathione and thioredoxin, antioxidant defense, redox regulation, and donation of reducing equivalents to other enzymes including ribonucleotide reductase, glutathione S-transferase, glyoxalases, and peroxidases (1–4). As mentioned above, numerous organisms including *Drosophila melanogaster* and *Anopheles* do completely lack a genuine GR. In these insects, glutathione reduction is maintained by the thioredoxin system (6, 25). As recently shown, also humans with inherited complete GR deficiency can live an almost normal life (26). Moreover, *P. falciparum* efficiently invades and develops inside GR-deficient erythrocytes (27). These observations further support the notion of a functional compensation by the thioredoxin system. Indeed, apart from thioredoxin, also plasmoredoxin, and in many organisms glutaredoxin, have been shown to reduce ribonucleotide reductase, which catalyzes the first step of DNA and RNA synthesis (1, 23). As recently shown by Sturm *et al.* (28) using interactome analyses, also the redox regulatory properties of thioredoxin, glutaredoxin, and plasmoredoxin are largely overlapping. Furthermore, the peroxiredoxins acting in *Plasmodium* are mainly thioredoxin but also glutaredoxin dependent (1). Concentrations of total glutathione and non-protein bound free thiols were found to not differ significantly between WT and GR(–) or TrxR(–) blood stage parasites. This result supports the finding that the parasites are viable in the absence of either of the two disulfide reductases, and that glutathione and thiol homeostasis are not largely disturbed. Taken together, the available data suggest that in *P. berghei* blood stage parasites, GR and TrxR might be able to largely compensate for each other. In addition, we cannot exclude that reduction by dihydrolipoamide of glutaredoxins, and indirectly of glutathione disulfide and thioredoxin disulfide, can functionally replace the NADPH-dependent enzymes GR and TrxR (16, 29, 30).

Interfering with redox metabolism represents a promising approach to antiparasitic drug development (20) prominent examples being *Schistosoma mansoni* thioredoxin-glutathione reductase (31) and trypanothione reductase of *L. donovani* and *T.b. brucei* (32). Also *Plasmodium* GR was considered a leading drug target because (i) complete structural information, which permits computational inhibitor modeling, is available (33), (ii) detailed enzyme kinetic data provided the framework for high throughput inhibitor and mechanistic studies (34), and (iii) several antimalarial agents that presumably act against GR have been developed (18, 35, 36). TrxR was discussed as a promising enzymic drug target because (i) knockout data pointed toward essentiality of the enzyme for blood stage parasites (17), (ii) detailed mechanistic and kinetic properties of PfTrxR are known (Ref. 37, and references therein), (iii) structural differences between the selenoprotein hTrxR and PfTrxR occurring at the solvent exposed C-terminal end of the proteins were considered most attractive sites for directed inhibitor development (22, 37), and (iv) numerous PfTrxR inhibitors had been developed (38, 39).

According to our data in *P. berghei*, neither GR nor TrxR are essential for blood stage malaria parasites. In case the data should be transferable to *P. falciparum*, the potential of mere inhibitors of either disulfide reductase as drug candidate needs to be questioned. However, compounds inhibiting both, structurally highly related, disulfide reductases simultaneously and inhibitors acting on PfGR in mosquito stages should still be considered as antimalarial strategies. Furthermore, drugs like methylene blue that act as redox-cycling substrates of plasmodial GR or TrxR (18, 20) are still very promising.

---

*Acknowledgments*—We thank Olivier Silvie for critical comments on the manuscript. We are also indebted to Drs. Blandin Franke-Fayard and Chris J. Janse (Leiden) for continuous discussions and sharing unpublished results.

---

## REFERENCES

1. Becker, K., Koncarevic, S., and Hunt, N. H. (2005) in *Molecular Approaches to Malaria* (Sherman, I. W., ed), pp. 365–383, American Society of Microbiology, Washington D. C.
2. Müller, S. (2004) *Mol. Microbiol.* **53**, 1291–1305
3. Becker, K., Tilley, L., Vennerstrom, J. L., Roberts, D., Rogerson, S., and Ginsburg, H. (2004) *Int. J. Parasitol.* **34**, 163–189
4. Becker, K., Rahlfs, S., Nickel, C., and Schirmer, R. H. (2003) *Biol. Chem.* **384**, 551–566
5. Schirmer, R. H., Bauer, H., and Becker, K. (2002) in *Wiley Encyclopedia of Molecular Medicine* (Creighton, T. E., ed), pp. 1471–1476, John Wiley and Sons, New York, NY
6. Kanzok, S. M., Schirmer, R. H., Turbachova, I., Iozef, R., and Becker, K. (2000) *J. Biol. Chem.* **275**, 40180–40186
7. Krnajska, Z., Gilberger, T. W., Walter, R. D., and Müller, S. (2001) *Mol. Biochem. Parasitol.* **112**, 219–228
8. Nickel, C., Rahlfs, S., Deponte, M., Koncarevic, S., and Becker, K. (2006) *Antioxid. Redox Signal* **8**, 1227–1239
9. Fairlamb, A. H., and Cerami, A. (1992) *Annu. Rev. Microbiol.* **46**, 695–729
10. Krauth-Siegel, R. L., Meiering, S. K., and Schmidt, H. (2003) *Biol. Chem.* **384**, 539–549
11. Ridley, R. G. (2002) *Nature* **415**, 686–693
12. Sobolewski, P., Gramaglia, I., Frangos, J. A., Intaglietta, M., and van der Heyde, H. (2005) *Infect. Immun.* **73**, 6704–6710
13. Janse, C. J., Franke-Fayard, B., Mair, G. R., Ramesar, J., Thiel, C., Engelman, S., Matuschewski, K., van Gemert, G. J., Sauerwein, R. W., and Waters, A. P. (2006) *Mol. Biochem. Parasitol.* **145**, 60–70
14. Tsuji, M., Mattei, D., Nussenzweig, R. S., Eichinger, D., and Zavala, F. (1994) *Parasitol. Res.* **80**, 16–21
15. Becker, K., Gui, M., Traxler, A., Kirsten, C., and Schirmer, R. H. (1994) *Histochemistry.* **102**, 389–395
16. Ellman, G. L. (1959) *Arch. Biochem. Biophys.* **82**, 70–77
17. Krnajska, Z., Gilberger, T. W., Walter, R. D., Cowman, A. F., and Müller, S. (2002) *J. Biol. Chem.* **277**, 25970–25975
18. Buchholz, K., Schirmer, R. H., Eubel, J. K., Akoachere, M. B., Dandekar, T., Becker, K., and Gromer, S. (2008) *Antimicrob. Agents Chemother.* **52**, 183–191
19. Vega-Rodríguez, J., Franke-Fayard, B., Dinglasan, R. R., Janse, C. J., Pas-trana-Mena, R., Waters, A. P., Coppens, I., Rodríguez-Orengo, J. F., Srinivasan, P., Jacobs-Lorena, M., and Serrano, A. E. (2009) *PLoS Pathogens* **5**, e1000302
20. Krauth-Siegel, R. L., Bauer, H., and Schirmer, R. H. (2005) *Angew. Chem. Int. Ed. Engl.* **44**, 690–715
21. Luersen, K., Walter, R. D., and Müller, S. (2000) *Biochem. J.* **34**, 545–552
22. Rahlfs, S., and Becker, K. (2006) *Mini Rev. Med. Chem.* **6**, 163–176
23. Becker, K., Kanzok, S. M., Iozef, R., Fischer, M., Schirmer, R. H., and

- Rahlfs, S. (2003) *Eur. J. Biochem.* **270**, 1057–1064
24. Buchholz, K., Rahlfs, S., Schirmer, R. H., Becker, K., and Matuschewski, K. (2008) *PLoS One* **6**, e2474
  25. Kanzok, S. M., Fechner, A., Bauer, H., Ulschmid, J. K., Müller, H. M., Botella-Munoz, J., Schneuwly, S., Schirmer, R., and Becker, K. (2001) *Science* **291**, 643–646
  26. Kamerbeek, N. M., van Zwieten, R., de Boer, M., Morren, G., Vuil, H., Bannink, N., Lincke, C., Dolman, K. M., Becker, K., Schirmer, R. H., Gromer, S., and Roos, D. (2007) *Blood* **109**, 3560–3566
  27. Gallo, V., Schwarzer, E., Rahlfs, S., Schirmer, R. H., van Zwieten, R., Roos, D., Arese, P., and Becker, K. (2009) *PLoS One* **4**, e7303
  28. Sturm, N., Mailu, B. M., Jortzik, E., Koncarevic, S., Deponte, M., Forchhammer, K., Rahlfs, S., and Becker, K. (2009) *PLoS Pathogens* **5**, e10003
  29. Porras, P., Pedrajas, J. R., Martínez-Galisteo, E., Padilla, C. A., Johansson, C., Holmgren, A., and Bárcena, J. A. (2002) *Biochem. Biophys. Res. Commun.* **295**, 1046–1051
  30. McMillan, P. J., Stimmler, L. M., Foth, B. J., McFadden, G. I., and Müller, S. (2005) *Mol. Microbiol.* **55**, 27–38
  31. Kuntz, A. N., Davioud-Charvet, E., Sayed, A. A., Califf, L. L., Dessolin, J., Arnér, E. S., and Williams, D. L. (2007) *PLoS Med.* **4**, e206
  32. Krieger, S., Schwarz, W., Ariyanayagam, M. R., Fairlamb, A. H., Krauth-Siegel, R. L., and Clayton, C. (2000) *Mol. Microbiol.* **35**, 542–552
  33. Sarma, G. N., Savvides, S. N., Becker, K., Schirmer, M., Schirmer, R. H., and Karplus, P. A. (2003) *J. Mol. Biol.* **328**, 893–907
  34. Krauth-Siegel, R. L., Müller, J. G., Lottspeich, F., and Schirmer, R. H. (1996) *Eur. J. Biochem.* **235**, 345–350
  35. Davioud-Charvet, E., Delarue, S., Biot, C., Schwöbel, B., Boehme, C. C., Müssigbrodt, A., Maes, L., Sergheraert, C., Grellier, P., Schirmer, R. H., and Becker, K. (2001) *J. Med. Chem.* **44**, 4268–4276
  36. Friebolin, W., Jannack, B., Wenzel, N., Furrer, J., Oeser, T., Sanchez, C. P., Lanzer, M., Yardley, V., Becker, K., and Davioud-Charvet, E. (2008) *J. Med. Chem.* **51**, 1260–1277
  37. McMillan, P. J., Arscott, L. D., Ballou, D. P., Becker, K., Williams, C. H., Jr., and Müller, S. (2006) *J. Biol. Chem.* **281**, 32967–32977
  38. Andricopulo, A. D., Akoachere, M. B., Krogh, R., Nickel, C., McLeish, M. J., Kenyon, G. L., Ascott, L. D., Williams, C. H., Jr., Davioud-Charvet, E., and Becker, K. (2006) *Bioorg. Med. Chem. Lett.* **16**, 2283–2292
  39. Morin, C., Besset, T., Moutet, I. C., Fayolle, M., Brückner, M., Limosin, D., Becker, K., and Davioud-Charvet, E. (2008) *Org. Biomol. Chem.* **6**, 2731–2742